Environ. Sci. Technol. **2004**, *38,* 674−681

Direct Speciation of Phosphorus in Alum-Amended Poultry Litter: Solid-State ^{31}P NMR Investigation

STEFAN HUNGER,*,† HERMAN CHO,‡ JAMES T. SIMS,§ AND DONALD L. SPARKS§

School of Earth Sciences, University of Leeds, Leeds LS2 9JT, United Kingdom, Environmental Molecular Sciences Laboratory, Pacific Northwest National Laboratory, Richland, Washington 99352, and Department of Plant and Soil Sciences, University of Delaware, Newark, Delaware 19717

Amending poultry litter (PL) with aluminum sulfate (alum) has proven to be effective in reducing water-soluble phosphorus (P) in the litter and in runoff from fields that have received PL applications; it has therefore been suggested as a best management practice. Although its effectiveness has been demonstrated on a macroscopic scale in the field, little is known about P speciation in either alum-amended or unamended litter. This knowledge is important for the evaluation of the long-term stability and bioavailability of P, which is a necessary prerequisite for the assessment of the sustainability of intensive poultry operations. Both solid-state MAS and CP-MAS ^{31}P NMR as well as ^{31}P{^{27}Al}-TRAPDOR were used to investigate P speciation in alum-amended and unamended PL. The results indicate the presence of a complex mixture of organic and inorganic orthophosphate phases. A calcium phosphate phase, probably a surface precipitate on calcium carbonate, could be identified in both unamended and alum-amended PL, as well as physically bound HPO_4^{2-}. Phosphate associated with Al was found in the alum-amended PL, most probably a mixture of a poorly ordered wavellite and phosphate surface complexes on aluminum hydroxide that had been formed by the hydrolysis of alum. However, a complex mixture of organic and inorganic phosphate species could not be resolved. Phosphate associated with Al comprised on average 40 ± 14% of the total P in alum-amended PL, whereas calcium phosphate phases comprised on average 7 ± 4% in the alum-amended PL and 14 ± 5% in the unamended PL.

Introduction

Phosphorus (P) has been recognized as the limiting nutrient for eutrophication in fresh waters. Although a naturally occurring aging phenomenon of surface water, eutrophication is accelerated by anthropogenic nutrient inputs and therefore poses a severe threat to water quality worldwide (*1*−*3*). Elevated concentrations of phosphorus have also been linked to the outbreak of the dinoflagellate *Pfiesteria piscicida* in estuaries on the Atlantic coast of the United States, which produces a toxin lethal to fish and hazardous to the health of humans (*4*−*6*). With globally diminishing fresh-water supplies and the accompanying political and social problems expected or already encountered worldwide, the management and protection of fresh-water supplies have become environmental challenges for the immediate future and play an important role toward sustainable development. After decades of regulating point-sources and decreasing P inputs into lakes, streams, and estuaries from industry and municipal wastewater treatment plants, inputs of P from agriculture have remained as an important non-point-source.

Agriculture relies on the application of nutrients to soils to enhance food production. Animal manures have especially proven to be an inexpensive and effective way to improve soil quality and agricultural productivity. However, in areas with extensive animal operations, the amounts of animal manure that must be disposed of have led to the overapplication of fertilizers, especially P. Phosphorus can be lost from soils by erosion (particulate P) and by surface runoff and leaching (primarily soluble P).

To reduce the negative effects of overapplication of animal manures in agriculture, efforts have been made to reduce the amount of water-soluble P in animal manures. A promising approach is the addition of chemical amendments, such as lime, ferric chloride, or alum (aluminum sulfate hydrate) (*7*, *8*). Alum has received particular interest in the treatment of poultry litter (PL) for its effectiveness in reducing the amount of water-soluble P while at the same time preventing loss of nitrogen (N) by ammonia volatilization, which diminishes air quality as well as the quality of the litter as fertilizer (*9*, *10*). Alum has also been shown to be effective in reducing water-soluble metal concentrations in PL (*11*, *12*).

Although the effectiveness of alum as an amendment for PL has been proven on a macroscopic scale in poultry houses and in the field, the types of reactions of phosphate in the alum-amended and unamended litter have been speculative. Initially, it was assumed that phosphate in animal manures reacts with Al^{3+} to form solid aluminum phosphate (*8*), which is insoluble in the pH range typical for agricultural soils (*13*). Although this assumption has been recognized as oversimplified (e.g., ref *14*), little, if any, information about the mechanisms of P fixation in PL is available, mainly due to the lack of methods sufficiently sensitive to directly determine the species, or form of P, in heterogeneous materials such as PL and soil. Recently, an X-ray absorption near edge structure (XANES) spectroscopic study of PL conducted in our research group (*15*) showed the presence of a calcium phosphate phase in the unamended PL samples, whereas features in the XANES spectra of the alum-amended PL samples indicated the formation of a P species similar to phosphate adsorbed to aluminum hydroxide.

Recent advances in nuclear magnetic resonance (NMR) spectroscopy have made it a versatile technique in soil and environmental sciences research (*16*, *17*). NMR spectroscopy is sensitive to the direct chemical environment of the investigated nucleus and does not require crystalline samples, which makes it an ideal technique to study molecular species in heterogeneous matrices.

Liquid-state NMR has been used to characterize P species in extracts of soils (*18*−*26*), wastewater sludge (biosolids) (*27*, *28*), and animal manures (*29*, *30*). Although this method has advanced our understanding of the transformation and mineralization of organic phosphates in soils, animal ma-

* Corresponding author phone: +44-113-343-6623; fax: +44-113-343-5259; e-mail: s.hunger@earth.leeds.ac.uk.
† University of Leeds.
‡ Pacific Northwest National Laboratory.
§ University of Delaware.

10.1021/es034755s CCC: $27.50
Published on Web 12/19/2003

nures, and biosolids, the possibility of the creation of artifacts by hydrolysis during the extraction steps makes a less invasive technique desirable.

High-resolution solid-state NMR spectroscopy is an important noninvasive tool to provide specific information about elemental speciation in amorphous and/or heterogeneous matrices. Using ^{31}P magic angle spinning (MAS) NMR, Hinedi and co-workers (*31*, *32*) identified calcium phosphate, aluminum phosphate, and pyrophosphate solid phases in anaerobically digested sewage sludge and soils amended with these biosolids. They also observed, however, that phosphate species in close contact with paramagnetic cations could not be accounted for due to the broadening of the NMR signals, a commonly encountered problem in NMR spectroscopy of soils (*33*).

Frossard and co-workers (*34*) characterized urban sewage sludge by sequential chemical fractionation with consecutive solid-state ^{31}P NMR analysis of the residual solids. They found that a complex mixture of phosphate solids was present in the sludge, including several calcium phosphates and aluminum phosphate.

Duffy and vanLoon (*14*) investigated the Al and P speciation in sewage sludge by comparing it with aluminum hydroxyl phosphates aged for different times using solid-state ^{31}P and ^{27}Al NMR spectroscopy. They found that phosphate species associated with aluminum generally have ^{31}P chemical shifts in the range from −7 to −30 ppm, with the less condensed aluminum phosphate polymers appearing at the higher end of this range. This broad range of reported chemical shifts requires a technique sensitive for dipolar coupling between P nuclei and Al nuclei to unambiguously assign peaks arising from the interaction between these spin pairs.

^{31}P{X} TRAPDOR has been used to directly probe the P−X connectivities (where X is a quadrupolar nucleus, e.g., ^{27}Al, ^{23}Na, or ^{11}B) in amorphous or microcrystalline materials, such as glasses and catalyst precursors. Using ^{31}P{^{27}Al } TRAPDOR, van Eck and co-workers (*35*) were able to show that a surface layer of $AlPO_4$ rather than one of phosphate polymers is formed on γ-Al_2O_3 during impregnation with phosphate. The complex ^{31}P NMR spectra of sodium aluminophosphate glasses (*36*), phosphate-containing aluminosilicate (*37*), and aluminoborosilicate glasses (*38*) could be conclusively interpreted by identifying phosphate species directly bound to Al, Na, or B.

In our research, high-resolution solid-state ^{31}P NMR spectroscopy was used to investigate and identify P species in alum-amended and unamended PL samples. Single-pulse excitation with proton decoupling during detection, ^{31}P{^{1}H}-CP-MAS, and ^{31}P{^{27}Al} TRAPDOR NMR were used to selectively enhance the signals of different phosphorus species and aid their identification.

Materials and Methods

Sample Preparation. Samples of PL were obtained from an on-farm evaluation of the effectiveness of alum as an amendment for PL. The details of this study were reported elsewhere (*12*). In brief, 194 poultry houses were chosen, of which 97 received alum and 97 served as a control group. The alum was applied and incorporated at an average rate of 90 g of alum per bird shortly after the previous flock and the upper crust of litter had been removed (approximately every 5−6 weeks). Samples were collected from the entire depth of the litter layer after the removal of the last flock in the study and then homogenized. Subsamples were dried at 65 °C and ground to pass an 0.8 mm screen. One sample (PL 181) was freeze-dried after 2 years of storage at 4 °C, ground using a mortar and pestle, and separated using standard mesh sieves into three size fractions (841−420, 420−125, and <125 μm). Containing the highest Al and P concentrations, the fine fraction (<125 μm) was used for the TRAPDOR experiments.

TABLE 1. Selected Properties of the Poultry Litter Samples Used in the NMR Studies

poultry litter sample[a]	pH[b]	total P %[c]	total Al %[c]	water soluble P[d] (mg kg^{-1})	water soluble Al[d] (mg kg^{-1})
PL 125	7.23	1.97	1.77	322	18.9
PL 134	7.37	2.32	1.09	783	23.1
PL 182	7.03	1.94	1.63	1167	19.5
PL 191	6.89	1.91	2.16	542	18.8
PL 197	7.32	2.09	1.54	355	18.7
PL 181 (<125 μm)	ND[e]	2.31	3.30	1050	0
PL 502	7.82	1.94	0.08	1635	2.5
PL 511	7.6	1.99	0.12	1754	1.6
PL 541	8.23	1.96	0.10	1308	6.1
PL 559	8.21	2.08	0.10	1570	7.9
PL 597	7.73	2.14	0.09	2534	2.7

[a] Samples 125−197 are alum-amended; samples 502−597 are unamended. [b] Determined as a suspension in DI water (litter-to-water ratio 1:4). [c] Total P and Al are given in wt % of the dry samples, determined by ICP-AES after digestion. [d] Water-soluble P and Al were determined by ICP-AES after extraction with DI water (fresh litter-to-water ratio 1:10). [e] Not determined.

Total Al and P concentrations were determined after microwave-assisted digestion with concentrated HNO_3 and 30% H_2O_2 (EPA 3051); water-soluble Al and P were determined after extraction of the fresh litter sample with deionized (DI) water (1:10 w/v) and filtering the extract through a 0.45 mm Supor filter (Gelman Laboratories, Ann Arbor, MI). Some of the extracted samples were freeze-dried and also used for NMR analysis. Phosphorus concentrations were measured by inductively coupled plasma atomic emission spectroscopy (ICP-AES) and using the colorimetric method described by Murphy and Riley (*39*). Aluminum concentrations were determined using ICP-AES. Sample pH was determined in suspension in DI water, using a 1:4 PL to water ratio. Selected properties of the samples are listed in Table 1. The water content of the samples after drying was estimated by thermogravimetric analysis (TGA) using a Hi-Res TGA 2950 thermogravimetric analyzer (TA Instrumtents, New Castle, DE). The initial, continuous weight loss up to a temperature of 150 °C was attributed to the evaporation of water (*40*).

Reference phosphate compounds were purchased and analyzed for comparison. $CaHPO_4$ and $Ca_5(PO_4)_3OH$ were purchased from Fisher Scientific (Fair Lawn, NJ). Calcium phytate and sodium phytate were purchased from Aldrich. Mineral samples of wavellite [$Al_3(OH)_3(PO_4)\cdot 2H_2O$] and variscite ($AlPO_4\cdot 2H_2O$) were provided by the Excalibur Mineral Co.

NMR Experiments. Solid-state ^{31}P NMR spectra were recorded on a Chemagnetics CMX Infinity spectrometer with an Oxford 300 MHz wide-bore magnet operating at a magnetic field of 7.04 T, corresponding to resonance frequencies of 78.16 MHz for ^{27}Al, 121.4 MHz for ^{31}P, and 299.9 MHz for ^{1}H. To afford uniform distribution and homogeneous spinning of the rotor in the MAS probe, dried and ground samples were used. Spinning speeds were maintained constant at values from 7 to 10 kHz ± 5 Hz.

CP-MAS experiments used a proton $\pi/2$ pulse of 3.5 μs, a contact time of 1.3 ms, and a pulse delay of 2 s. Depending on the P concentration, 2000−4000 scans were accumulated to give a signal-to-noise ratio of at least 30:1. Single-pulse, proton-decoupled spectra were recorded using a ^{31}P $\pi/2$ pulse of 3.7 μs and a relaxation delay of 60 s. For these experiments up to 512 scans were accumulated.

The ^{31}P{^{27}Al} TRAPDOR pulse sequence acquires two ^{31}P echo spectra, of which the first spectrum serves as a reference

(*37*). During the evolution of the second echo, a radio frequency is applied to the ^{27}Al channel, which facilitates relaxation of the P nuclei in close proximity via dipolar coupling. The difference of the two spectra shows the peaks of P nuclei that are in close proximity to Al nuclei. The dephasing time, during which radio frequency is applied to the ^{27}Al channel, was determined in a set of preliminary experiments. We found that employing a dephasing time of 2−3 ms is most effective but that signal intensity is also lost during this time due to relaxation via pathways other than dipolar decoupling. A dephasing time of 1.6 ms showed the best TRAPDOR effect while retaining maximum signal intensity in the standard sample. The echo spectra were recorded using ^{31}P $\pi/2$ and π pulses of 3.45 and 6.9 μs, respectively, proton-decoupling during acquisition, and a pulse delay of 30 s between the sequences. At least 1000 scans were accumulated, and the echo spectra with and without dephasing were processed separately.

The spectra were processed using the NUTS NMR utility transform software by Acorn NMR. A line broadening of 50−100 Hz was applied prior to Fourier transformation and phase correction. The complex signals were deconvoluted using a minimal set of peaks. The quality of the fit increased when Lorentzian peaks for narrow peaks and Gaussian peaks for broad peaks were used. No other constraints were employed. Isotropic chemical shifts are all reported in parts per million (ppm) relative to the peak of 85% H_3PO_4 as an external reference; positive values correspond to low-field or high-frequency shifts. All spectra have been normalized to the most intense peak.

Results and Discussion

Poultry feed contains dicalcium phosphate (DCP) and calcium carbonate, which dissolve during digestion; both calcium and phosphate ions will be partially excreted in some form. Because poultry lack the enzymes necessary to hydrolyze the phytic acid contained in the grain that makes up most of their diet, poultry manure and litter have therefore long been known to contain phytic acid (*41*). The PL consists of the feces and the bedding material, mainly wood chips and sawdust, and has neutral to slightly basic pH values (Table 1). In the alum-amended litter (Table 1, samples PL 125−197), the pH initially dropped to pH 5−5.5 after the addition of alum and slowly increased over time as more feces were added, reaching values slightly lower than those of the unamended litter (Table 1, samples PL 502−597) (*12*).

Considering the elemental composition and the pH of PL (*9*, *12*, *42*), P chemistry was expected to be dominated by interactions with Al (in the amended samples), Ca, and Mg and by organic phosphate (e.g., undigested phytic acid and compounds derived from metabolic processes). Other components in PL that are expected to form stable compounds with P are Fe, Mn, and Zn. In solid-state ^{31}P NMR spectroscopy, calcium, magnesium, and aluminum phosphate compounds have characteristic isotropic chemical shifts (*43*−*46*). Iron and manganese phosphate compounds are not expected to be detected in the spectra because of paramagnetic line-broadening (*32*, *47*, *48*). The chemical shifts of the more soluble phosphate salts with various cations (Na, K, NH_4, etc.) are also reported (*49*, *50*), but those are not expected to form as crystalline phases at high humidity and in the presence of cations forming less soluble compounds. However, by forming complexes with organic and inorganic phosphate, these cations change the electron density in the phosphate anion and are therefore expected to influence the chemical shift of the ^{31}P nucleus (*50*).

The single-pulse MAS NMR spectra of both the unamended (Figure 1) and alum-amended samples (Figure 2) show broad, complex resonances centered at 0 ppm. The range of chemical shifts observed in these spectra confirms

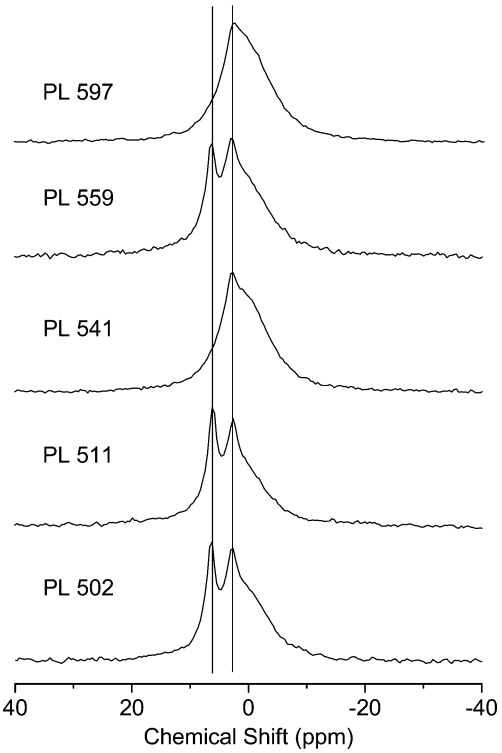

FIGURE 1. Single-pulse, proton-decoupled ^{31}P MAS NMR spectra of unamended PL samples. Chemical shifts of the marked peaks are 6.4 and 2.8 ppm; for discussion see text.

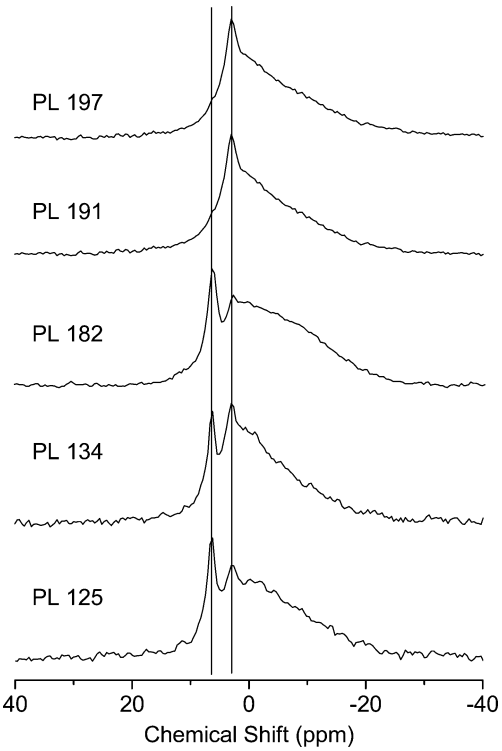

FIGURE 2. Single-pulse, proton-decoupled ^{31}P MAS NMR spectra of alum-amended PL samples. Chemical shifts of the marked peaks are 6.4 and 2.8 ppm; for discussion see text.

a predominant oxidation state of P(V) in the PL, which has also been shown by Peak et al. (*15*). One or two relatively sharp peaks can be distinguished. Deconvolution of the signals is illustrated for sample PL 125 (alum-amended sample) in Figure 3. The complete deconvolution results are shown in Table 2. Deconvolution of the spectra reveals a set

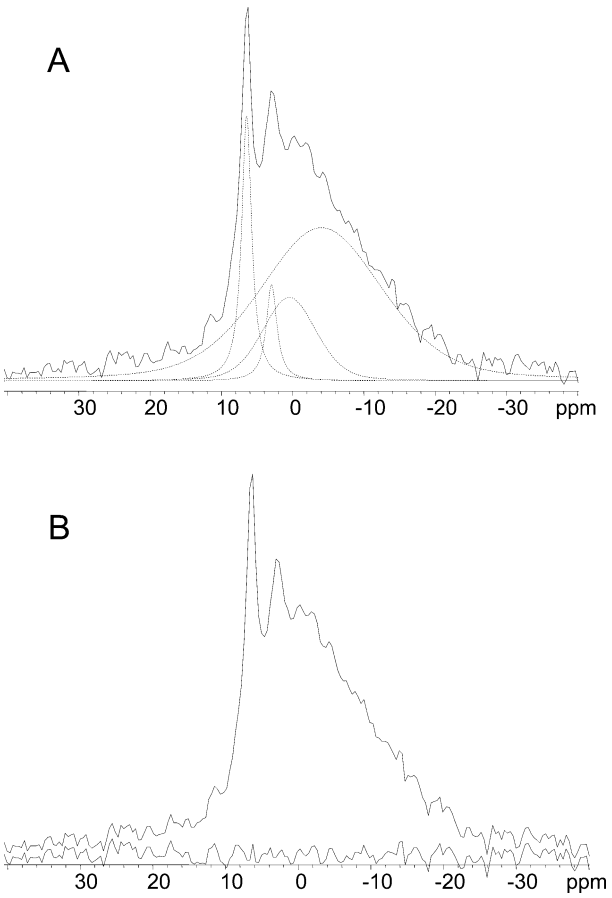

FIGURE 3. Deconvoluted single-pulse, proton-decoupled ^{31}P MAS NMR spectrum of sample PL 125: (A) (dashed lines) fitted peaks (6.4, 2.9, −0.3, and −4.4 ppm); (solid line) original data; (B) original data (top) and difference spectrum (bottom).

of up to four peaks, all of which are present in some of the alum-amended samples (samples PL 125, PL 134, and PL 182 in Figure 2), whereas in some unamended samples only two peaks are found (samples PL 541 and PL 597 in Figure 1). One sharp peak with a chemical shift of 2.8−3.0 ppm and varying intensity and a broad peak centered between −1 and 1 ppm are present in all of the samples investigated. Another sharp peak at 6.4 ppm can be found in most of the samples. The spectra of the alum-amended samples (Figure 2) are dominated by one very broad resonance of Gaussian line-shape centered between −4 and −10 ppm, which appears as a tailing on the negative side of the composite signal.

Comparison of the single-pulse MAS (Figures 1 and 2) and CP-MAS spectra (Figures 4 and 5) shows that the peak at 6.4 ppm is selectively enhanced by cross-polarization and that it is present in all samples but sample PL 541 (Figure 4). The peak at 2.8 ppm, on the other hand, is suppressed in the CP spectra. The broad resonances at 0 and −4 to −10 ppm are also enhanced but less so than the intense peak at 6.4 ppm. Additionally, a weak resonance at −20 ppm can be detected in the cross-polarized spectra of two of the unamended samples (samples PL 511 and PL 541; see enlarged spectra in Figure 4) and of two of the alum-amended samples (samples PL 125 and PL 182; see enlarged spectra in Figure 5). This peak is an artifact that can be traced to a contamination of the rotor with a small amount of variscite ($AlPO_4 \cdot 2H_2O$).

The CP-MAS pulse sequence transfers magnetization from protons to the investigated nucleus in close proximity, in this case P, selectively enhancing the resonance signal (*51*, *52*). The selective enhancement of the peak at 6.4 ppm in the CP-MAS spectra indicates that it is either a protonated or hydrogen-bonded phosphate species or a solid phosphate phase with protons in fixed crystallographic positions in close proximity to phosphate. This species further has a very uniform chemical environment, as indicated by the narrow line-width. A chemical shift of 6.6 ppm has been reported for crystalline Na_2HPO_4 by Turner and co-workers (*50*). Although sodium is present in PL (*8*, *42*, *53*), the formation of a solid sodium phosphate of sufficient crystallinity to give a signal as narrow as the one observed in the spectra is very unlikely due to the heterogeneity of the material. Sodium phosphate is quite soluble, and it is not expected to precipitate in the presence of Ca, Mg, and Fe, which are also found in PL (*8*, *42*, *53*) and form less soluble solids with phosphate.

In alkaline extracts of soils and manures, the chemical shift of inorganic orthophosphate has been reported to be 6.3−6.5 ppm (*18*, *19*, *29*). The chemical shift of phosphate in aqueous solutions is sensitive to the pH and ranges from 0 ppm for H_3PO_4 (by definition) through 8 ppm for PO_4^{3-} (*54*, *55*), with HPO_4^{2-} appearing at ~6 ppm. Although the absolute water content of the samples used for the NMR experiments was considerably less in comparison with the PL in situ (30−35%) due to drying at 65 °C, no attempt was made to completely remove all water. The water content of the samples (~10%, determined by TGA) is therefore sufficient for the physically adsorbed HPO_4^{2-} to retain water of hydration inside the organic matrix. Unfortunately, no reference data exist for these phosphate species. Although it has not been established whether chemical shifts in solids can be directly compared to those in the liquid state, results from solution NMR experiments can be helpful in identifying

TABLE 2. Deconvolution Results of the Single-Pulse, Proton-Decoupled ^{31}P MAS NMR Spectra

sample	peak	chemical shift (ppm)	relative height (% of peak 3)	width (Hz)	relative peak area (%)
PL 125	1	6.44	284	356	10.69
	2	2.98	110	302	5.34
	3	−0.68	100	1517	58.72
	4	−10.53	157	1726	25.25
PL 134	1	6.47	150	213	5.77
	2	3.09	98.4	235	3.99
	3	1.35	100	1378	62.89
	4	−7.73	114	1891	27.36
PL 182	1	6.27	374	221	6.75
	2	2.55	114	190	1.27
	3	2	100	1358	28.13
	4	−6.42	260	2228	63.85
PL 191	2	2.79	119	346	12.76
	3	0.79	100	1080	40.77
	4	−7.19	68.8	1780	46.47
PL 197	2	3.1	180	277	10.39
	3	1.07	100	1381	53.02
	4	−8.52	138	2020	36.59
PL 502	1	6.51	136	191	13.49
	2	2.8	77.7	207	8.08
	3	1.2	100	1348	78.43
PL 511	1	6.16	209	209	17.39
	2	2.67	142	224	10.14
	3	1.27	100	1224	72.46
PL 541	2	2.98	51.9	407	18.03
	3	−0.11	100	1209	81.97
PL 559	1	6.44	77.3	230	11.1
	2	2.97	46.6	252	7.27
	3	1.49	100	1311	81.63
PL 597	2	2.6	63	446	18.7
	3	−0.3	100	1224	81.3

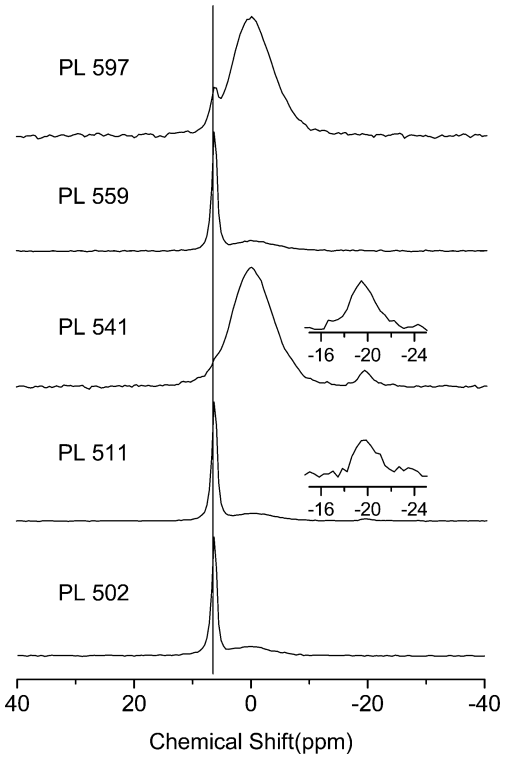

FIGURE 4. CP-MAS ^{31}P NMR spectra of unamended PL samples. Insets show enlargements of the chemical shift region indicated. The chemical shift of the marked peak is 6.4 ppm; for discussion see text.

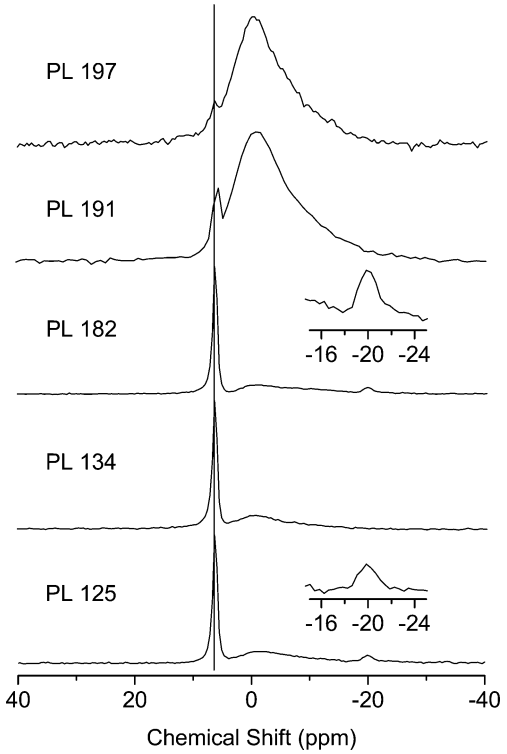

FIGURE 5. CP-MAS ^{31}P NMR spectra of alum-amended PL samples. Insets show enlargements of the chemical shift region indicated. Chemical shift of the marked peak is 6.4 ppm; for discussion see text.

species in PL. Although P chemical shifts in crystalline and amorphous homogeneous solid phases are influenced by the cations present for charge balance (*50*), this effect will be less pronounced for phosphate species in an organic matrix, due to complexation of the cations with the organic material and a considerably less uniform complexation environment for phosphate.

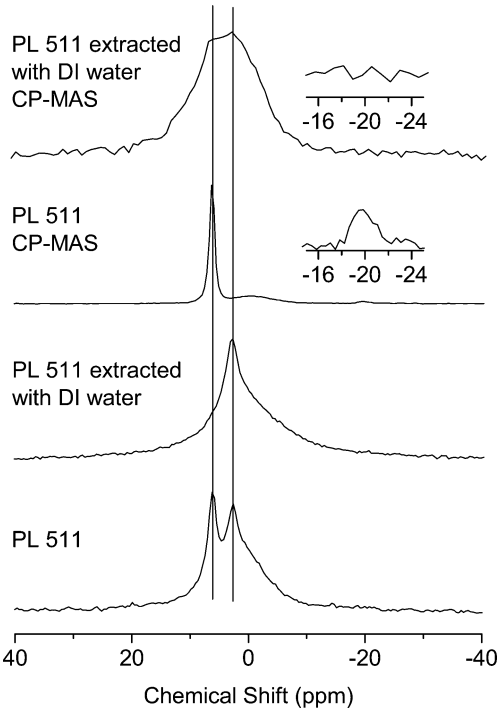

FIGURE 6. ^{31}P MAS NMR spectra of unamended sample 511, before and after extraction with DI water. Insets show enlargements of the chemical shift region indicated. Chemical shifts of the marked peaks are 6.4 and 2.8 ppm; for discussion see text.

Considering the narrow line-width despite the complexity of the material, and the chemical shift, it is therefore concluded that the signal at 6.4 ppm corresponds to inorganic HPO_4^{2-} bound by hydrogen bonds to physically adsorbed water. This interpretation is supported by the fact that the peak disappears upon extraction with water, which indicates that the species is readily water-soluble (compare Figure 6). In the following discussion, this phosphate fraction is referred to as being physically adsorbed.

A phosphorus XANES spectroscopic study of the PL samples used in our study without prior drying indicated the presence of a calcium phosphate phase characterized as dicalcium phosphate (*15*). Similar to ^{31}P NMR spectroscopy, P-XANES spectroscopy is element-specific and sensitive to the direct chemical environment of the investigated nucleus and can be used to analyze amorphous samples.

Chemical shifts for several crystalline calcium phosphate phases have been reported, ranging from −1.5 and 0 ppm in anhydrous dicalcium phosphate (DCPA, monetite), 1.7 ppm in dicalcium phosphate dihydrate (DCPD, brushite), and −0.2 and 3.4 ppm in octacalcium phosphate (OCP) to 2.8 to 3.0 ppm in hydroxyl apatite (HAP) (*43*, *56*) as well as in tribasic calcium phosphate (*50*). The chemical shift of a calcium phosphate phase formed at the surface of calcite in aqueous suspension was also reported at 3.0 ppm (*57*).

In general, the phosphate peaks shifted to more negative values are attributed to protonated phosphate anions, whereas the peaks shifted to more positive values are attributed to deprotonated species (*43*), which corresponds to the trend of phosphate chemical shifts in aqueous solution (*54*). Phosphate species in calcium phosphate phases, which are characterized by chemical shifts of 2.8−3.4 ppm, are referred to as being located in "apatitic" layers (*43*), that is, showing a local chemical environment similar to HAP.

The less stable compounds DCP and OCP typically hydrolyze to eventually form HAP (*13*). Inskeep (*58*) and

Grossl (*59*), however, found that this process is retarded in the presence of various organic acids, such as citric acid, tannic acid, or humic and fulvic acids. They suggested that organic acids adsorb to growth sites of the DCP and OCP crystals, efficiently inhibiting the transformation to HAP. Because PL contains a wide array of organic acids, the formation of a crystalline apatite is thus very unlikely.

Calcium carbonate forms under open atmosphere conditions when the pH of the litter increases after the initial decrease with addition of alum to the litter. It is also part of the chicken feed and therefore easily transferred to the litter. Phosphate sorbs strongly to calcium carbonate, and the chemical shift of the phosphate phase formed at the surface has been reported at 2.8 ppm (*57*).

Because formation of crystalline HAP is not expected in the litter, the most likely calcium phosphate phases corresponding to the peak at 2.9 ± 0.1 ppm would therefore be a tribasic calcium phosphate [$Ca_3(PO_4)_2$] or a calcium phosphate surface precipitate on calcium carbonate (*57*).

Chemical shift values for magnesium phosphate phases have been published. The naturally occurring crystalline compounds bobierrite [$Mg_3(PO_4)_2 \cdot 8\ H_2O$] and newberyite ($MgHPO_4 \cdot 3\ H_2O$) have chemical shifts of 4.6 and −7.2 ppm, respectively, and the amorphous compounds $Mg_3(PO_4)_2$ and $MgHPO_4$ have chemical shifts of 0.5 and −2.4 ppm, respectively (*45*, *46*). The crystalline magnesium phosphate phases and amorphous $MgHPO_4$ can be eliminated because of the absence of resonance signals in the appropriate chemical shift range. Although amorphous $Mg_3(PO_4)_2$ cannot be excluded, positive evidence cannot be presented from the NMR spectra alone, because its NMR peak (0.5 ppm) would be masked by the broad resonance at ∼0 ppm.

Chemical shifts of various aluminum phosphate solids are reported in the literature (*14*, *32*, *44*, *60*). Depending on crystallinity, water content, and degree of condensation, the phosphorus nuclei in these solids resonate between −7 and −30 ppm. Duffy and vanLoon (*14*) reported more negative shifts for aluminum phosphate precipitates that had been calcined and had therefore a higher degree of condensation. These findings are corroborated by simulations of NMR spectra of aluminum phosphate glasses (*61*), which indicate that phosphate peaks shift to more negative values with increasing number of aluminum atoms bound. Furthermore, phosphorus peaks shift to more negative values with decreasing pH. These two trends occur simultaneously and are very likely to be indistinguishable from each other. The minerals wavellite [$Al_3(OH)_3(PO_4)_2 \cdot 5\ H_2O$] (*62*) and variscite ($AlPO_4 \cdot 2H_2O$) (*63*), which were included in our study, had chemical shifts of −11 and −19 ppm, respectively, in agreement with published values (*34*, *44*). The chemical shift of berlinite ($AlPO_4$) has been reported at −25 ppm (*44*).

Lacking any sharp peaks at chemical shifts below 0 ppm, the alum-amended PL samples clearly do not contain any crystalline aluminum phosphate species. The main difference between the spectra of the alum-amended and the unamended samples is an additional broad peak centered between −4 and −10 ppm in the spectra of the former, which appears as a tailing on the negative side of the composite NMR signals. The broad line-width indicates that phosphate exists in this species in a distribution of chemical environments. The fact that this species is present only in the alum-amended samples indicates that it is probably an aluminum phosphate phase. To corroborate this hypothesis, a TRAPDOR experiment was conducted.

In Figure 7, the single-pulse spectrum of sample PL 181 is compared with the echo spectra with and without irradiation of the ^{27}Al nuclei and with the difference spectrum. The differences between the single-pulse spectrum and the echo spectrum can be attributed to different transversal relaxation times of the various phosphate species (*64*).

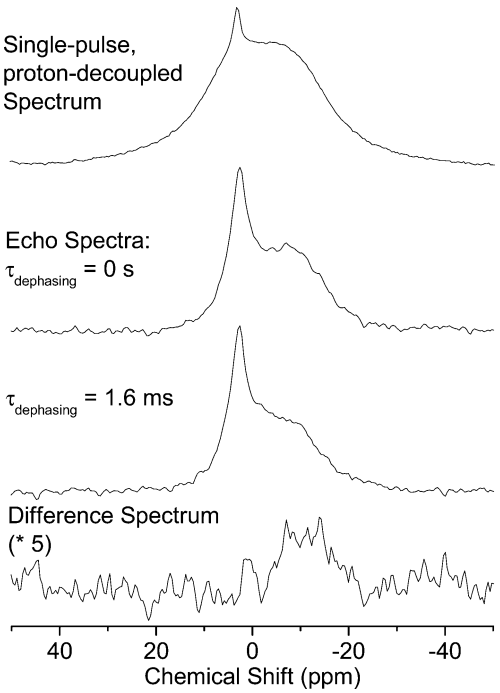

FIGURE 7. (Top) Single-pulse, proton-decoupled spectrum of PL sample 181 (<125 μm); (middle) echo spectra with and without dephasing; (bottom) difference spectrum, enlarged by a factor of ×5.

Comparison of the echo spectrum without dephasing with the one with $\tau_{dephasing} = 1.596$ ms reveals a reduction in peak height upon dephasing, which is shown more clearly in the difference spectrum. The difference spectrum shows a broad peak centered at δ −10, which indicates a heterogeneous chemical environment of the phosphate anions associated with aluminum. The chemical shift region is characteristic for aluminum phosphate species with a low degree of condensation (*14*). Possible structures are mononuclear and binuclear inner-sphere surface complexes of phosphate on aluminum hydroxide (*65*) or a poorly ordered, uncondensed aluminum phosphate polymer with a structure similar to that of wavellite. In wavellite, chains of corner-sharing $Al(OH)_6$ octahedra are cross-linked by phosphate. Crystalline wavellite was not observed in the XANES spectra of the PL samples (*15*).

At this point it is not yet possible to resolve the remaining complex resonances centered at ∼0 ppm. They are possibly due to organic orthophosphate species with a range of chemical environments and molecular conformations, which cause the broadening of the signal. Furthermore, as mentioned before, the chemical shift of inorganic orthophosphate is influenced by the cations it is complexed with. Turner and co-workers found a linear correlation between chemical shift and the electronegativity of the cations in several metal phosphates, with the less electronegative metals shifting the phosphate peaks to more positive values (*50*). The same trend can be seen for an organic phosphate species in the spectra of sodium and calcium phytate (Figure 8). Those two compounds were included in our study because phytic acid is known to be contained in poultry litter (*41*) and to illustrate the effect of the counterions on the chemical shift of P in phytic acid. Calcium phytate forms a crystalline phase with four magnetically nonequivalent phosphate groups, and its NMR spectrum can accordingly be resolved into four different peaks. Although sodium phytate is a crystalline phase as well, its phosphate groups are magnetically equivalent and cannot be deconvoluted. The change of the cation from calcium to sodium also caused the peaks to shift to more positive values.

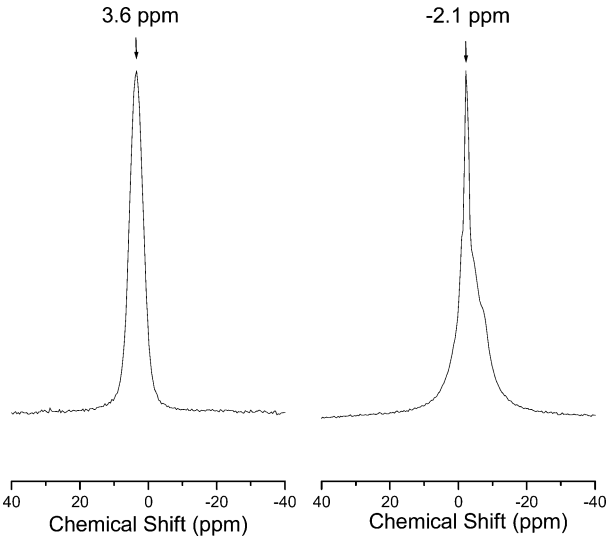

FIGURE 8. Single-pulse, proton-decoupled MAS NMR spectra of (left) sodium phytate and (right) calcium phytate.

The conclusions that can be drawn from these data are twofold: In the presence of a variety of cations, the organic orthophosphate species show broad, unresolved peaks. Furthermore, the presence of inorganic orthophosphate, which does not have a uniform environment like the physically adsorbed species (6.4 ppm), but rather forms complexes with a wide variety of cations, cannot be excluded. The inability to resolve these complex resonances shows clearly the limitations of solid-state ^{31}P NMR spectroscopy for the analysis of PL.

In the single-pulse, proton-decoupled ^{31}P NMR spectra, the signal intensities, which are measured as the peak areas, are approximately proportional to the relative concentrations. For minor peaks, however, deconvolution is not as exact as for the major peaks in a spectrum, and care must therefore be taken when interpreting signal intensities of peaks of low intensity. In general, an error margin of ±5% of the combined signal intensity of all signals is assumed for the peak areas of the deconvoluted spectra.

In the spectra of the alum-amended PL samples (Figure 2), the peak attributed to phosphate adsorbed to aluminum hydroxide or to an uncondensed aluminum phosphate (−4 to −10 ppm) contributes between 25 and 64% to the overall peak intensities. This clearly shows that on average 40 ± 14% of the total phosphate in the samples is bound in this manner and because of the strong covalent bond scarcely water-soluble.

The calcium phosphate phase, which is similarly insoluble in water, comprises on average 10 ± 5% of the total P in both alum-amended and unamended PL. Significantly less of the calcium phosphate phase is present in alum-amended PL (7 ± 4%) than in the unamended PL (14 ± 5%).

Only a minor proportion can be clearly identified as weakly bound inorganic orthophosphate and is expected to be readily water-soluble. However, some of the unresolved organic and inorganic orthophosphate species are soluble as well. Because it is impossible to deduce the exact proportion of these species, the quantitative solid-state NMR results cannot be used to predict the soluble phosphate proportion.

Our results show that solid-state ^{31}P NMR spectroscopy can be a valuable tool to identify some inorganic phosphate species in a heterogeneous material such as poultry litter. The identification of organic phosphate species, on the other hand, is not possible. A combination of solid-state and liquid-state ^{31}P NMR spectroscopy seems therefore most promising for a more complete analysis of poultry litter that includes the organic species, particularly phytic acid.

However accurate the P speciation of the PL samples by ^{31}P NMR might be, it shows only a picture representative of the P transformations in alum-amended or unamended PL over a short time. These transformations are likely to continue during storage of the material and in PL-amended soils over a longer time scale than considered here. Depending on the properties of the soils where alum-amended PL is applied, the climate, the management practices, and whether the PL is incorporated or applied to the surface, the P species found will transform at different rates.

A further investigation of the transformations of alum-amended PL over longer time scales is clearly needed to make scientifically sound recommendations on the use of alum-amended PL in agriculture and in contribution toward a more environmentally sustainable poultry industry. This work shows that ^{31}P NMR spectroscopy is an excellent spectroscopic tool to study P speciation and transformations in alum-amended and unamended poultry litter.

Acknowledgments

The NMR experiments were performed in the Environmental Molecular Sciences Laboratory (EMSL; a national scientific user facility sponsored by the U.S. DOE Office of Biological and Environmental Research) located at Pacific Northwest National Laboratory, operated by Battelle for the DOE. We especially appreciate the assistance of Dr. Sarah Burton and Dr. Joseph Ford in conducting the NMR experiments at EMSL. This paper benefited from valuable input from the Environmental Soil Chemistry research group of the University of Delaware. S.H. appreciates the support of a Delaware Water Resources Center graduate research fellowship.

Literature Cited

(1) Sharpley, A. N.; Daniel, T.; Sims, J. T.; Lemunyon, J.; Stevens, R.; Parry, R. *Agricultural Phosphorus and Eutrophication*; U.S. Department of Agriculture, U.S. GPO: Washington, DC, 1999.
(2) Sharpley, A. N.; Chapra, S. C.; Wedepohl, R.; Sims, J. T.; Daniel, T. C.; Reddy, K. R. *J. Environ. Qual.* **1994**, *23*, 437−451.
(3) Sharpley, A.; Foy, B.; Withers, P. *J. Environ. Qual.* **2000**, *29*, 1−9.
(4) Burkholder, J. M.; Noga, E. J.; Hobbs, C. H.; Glasgow Jr., H. B. *Nature* **1992**, *358*, 407−410.
(5) Burkholder, J. M.; Mallin, M. A.; Glasgow Jr., H. B.; Larsen, L. M.; McIver, M. R.; Shank, C.; Deamer-Melia, N.; Briley, D. S.; Springer, J.; Touchette, B. W.; Hannon, E. K. *J. Environ. Qual.* **1997**, *26*, 1451−1466.
(6) Burkholder, J. M.; Glasgow Jr., H. B. *Limnol. Oceanogr.* **1997**, *42*, 1052−1075.
(7) Moore Jr., P. A.; Daniel, T. C.; Edwards, D. R.; Miller, D. M. *J. Environ. Qual.* **1995**, *24*, 293−300.
(8) Moore Jr., P. A.; Miller, D. M. *J. Environ. Qual.* **1994**, *23*, 325−330.
(9) Moore Jr., P. A.; Daniel, T. C.; Edwards, D. R. *J. Environ. Qual.* **2000**, *29*, 37−49.
(10) Shreve, B. R.; Moore Jr., P. A.; Daniel, T. C.; Edwards, D. R.; Miller, D. M. *J. Environ. Qual.* **1995**, *24*, 106−111.
(11) Moore Jr., P. A.; Daniel, T. C.; Gilmour, J. T.; Shreve, B. R.; Edwards, D. R.; Wood, B. H. *J. Environ. Qual.* **1998**, *27*, 92−99.
(12) Sims, J. T.; Luka-McCafferty, N. J. *J. Environ. Qual.* **2002**, *31*, 2066−2073.
(13) Lindsay, W. L. *Chemical Equilibria in Soils*; John Wiley and Sons: New York, 1979.
(14) Duffy, S. J.; van Loon, G. W. *Can. J. Chem.* **1995**, *73*, 1645−1659.
(15) Peak, D.; Sims, J. T.; Sparks, D. L. *Environ. Sci. Technol.* **2002**, *36*, 4253−4261.
(16) Nanny, M. A.; Minear, R. A.; Leenheer, J. A. *Nuclear Magnetic Resonance Spectroscopy in Environmental Chemistry*; Oxford University Press: New York, 1997.
(17) Wilson, M. A. *NMR—Techniques and Applications in Geochemistry and Soil Chemistry*; Pergamon Press: Oxford, U.K., 1987.
(18) Cade-Menun, B. J.; Liu, C. W.; Nunlist, R.; McColl, J. G. *J. Environ. Qual.* **2002**, *31*, 457−465.
(19) Cade-Menun, B. J.; Preston, C. M. *Soil Sci.* **1996**, *161*, 770−785.
(20) Amelung, W.; Rodionov, A.; Urusevskaja, I. S.; Haumaier, L.; Zech, W. *Geoderma* **2001**, *103*, 335−350.
(21) Condron, L. M.; Goh, K. M.; Newman, R. H. *J. Soil Sci.* **1985**, *36*, 199−207.

(22) Mahieu, N.; Olk, D. C.; Randall, E. W. *Eur. J. Soil Sci.* **2000**, *51*, 391−402.
(23) Newman, R. H.; Tate, K. R. *Commun. Soil Sci. Plant Anal.* **1980**, *11*, 835−842.
(24) Pant, H. K.; Warman, P. R.; Nowak, J. *Commun. Soil Sci. Plant Anal.* **1999**, *30*, 757−772.
(25) Robinson, J. S.; Johnston, C. T.; Reddy, K. R. *Soil Sci.* **1998**, *163*, 705−713.
(26) Zhang, T. Q.; Mackenzie, A. F.; Sauriol, F. *Soil Sci.* **1999**, *164*, 662−670.
(27) Hinedi, Z. R.; Chang, A. C.; Lee, R. W. K. *J. Environ. Qual.* **1989**, *18*, 323−329.
(28) Hinedi, Z. R.; Chang, A. C.; Lee, R. W. K. *Soil Sci. Soc. Am. J.* **1988**, *52*, 1593−1596.
(29) Leinweber, P.; Haumaier, L.; Zech, W. *Biol. Fert. Soils* **1997**, *25*, 89−94.
(30) Crouse, D. A.; Sierzputowska-Gracz, H.; Mikkelsen, R. L. *Commun. Soil Sci. Plant Anal.* **2000**, *31*, 229−240.
(31) Hinedi, Z. R.; Chang, A. C. *Soil Sci. Soc. Am. J.* **1989**, *53*, 1057−1061.
(32) Hinedi, Z. R.; Chang, A. C.; Yesinowski, J. P. *Soil Sci. Soc. Am. J.* **1989**, *53*, 1053−1056.
(33) Smernik, R. J.; Oades, J. M. *J. Environ. Qual.* **2002**, *31*, 414−420.
(34) Frossard, E.; Tekely, P.; Grimal, J. Y. *Eur. J. Soil Sci.* **1994**, *45*, 403−408.
(35) van Eck, E. R. H.; Kentgens, A. P. M.; Kraus, H.; Prins, R. *J. Phys. Chem.* **1995**, *99*, 16080−16086.
(36) Lang, D. P.; Alam, T. M.; Bencoe, D. N. *Chem. Mater.* **2001**, *13*, 420−428.
(37) Schaller, T.; Rong, C.; Toplis, M. J.; Cho, H. *J. Non-Cryst. Solids* **1999**, *248*, 19−27.
(38) Rong, C.; Wong-Moon, K. C.; Li, H.; Hrma, P.; Cho, H. *J. Non-Cryst. Solids* **1998**, *223*, 32−42.
(39) Murphy, J.; Riley, H. P. *Anal. Chim. Acta* **1962**, *27*, 31−36.
(40) Widmann, G.; Riesen, R. *Thermoanalyse*, 3rd ed.; Hüthig: Heidelberg, Germany, 1990.
(41) Taylor, T. G. *P. Nutr. Soc.* **1965**, *24*, 105−112.
(42) Moore Jr., P. A.; Daniel, T. C.; Sharpley, A. N.; Wood, C. W. *J. Soil Water Conserv.* **1995**, *50*, 321−327.
(43) Elliott, J. C. *Structure and Chemistry of the Apatites and Other Calcium Orthophosphates*; Elsevier: Amsterdam, The Netherlands, 1994; Vol. 18.
(44) Bleam, W. F.; Pfeffer, P. E.; Freye, J. S. *Phys. Chem. Miner.* **1989**, *16*, 455−464.
(45) Aramendía, M. A.; Borau, V.; Jiménez, C.; Marinas, J. M.; Romero, F. J.; Ruiz, J. R. *J. Solid State Chem.* **1998**, *135*, 96−102.
(46) Aramendía, M. A.; Borau, V.; Jiménez, C.; Marinas, J. M.; Romero, F. J.; Ruiz, J. R. *J. Colloid Interface Sci.* **1998**, *202*, 456−461.
(47) Blumberg, W. E. *Phys. Rev.* **1960**, *119*, 79−84.
(48) Sutter, B.; Taylor, R. E.; Hossner, L. R.; Ming, D. W. *Soil Sci. Soc. Am. J.* **2002**, *66*, 455−463.
(49) Hartmann, P.; Vogel, J.; Schnabel, B. *J. Magn. Reson.* **1994**, *111*, 110−114.
(50) Turner, G. L.; Smith, K. A.; Kirkpatrick, R. J.; Oldfield, E. *J. Magn. Reson.* **1986**, *70*, 408−415.
(51) Pines, A.; Gibby, M. G.; Waugh, J. S. *J. Chem. Phys.* **1973**, *59*, 569−590.
(52) Hartmann, S. R.; Hahn, E. L. *Phys. Rev.* **1962**, *128*, 2042−2053.
(53) Jackson, B. P.; Bertsch, P. M.; Cabrera, M. L.; Camberato, J. J.; Seaman, J. C.; Wood, C. W. *J. Environ. Qual.* **2003**, *32*, 535−540.
(54) Mortlock, R. F.; Bell, A. T.; Radke, C. J. *J. Phys. Chem.* **1993**, *97*, 775−782.
(55) Yoza, N.; Ueda, N.; Nakashima, S. *Fresenius' J. Anal. Chem.* **1994**, *348*, 633−638.
(56) Rothwell, W. P.; Waugh, J. S.; Yesinowski, J. P. *J. Am. Chem. Soc.* **1980**, *102*, 2637−2643.
(57) Hinedi, Z. R.; Goldberg, S.; Chang, A. C.; Yesinowski, J. P. *J. Colloid Interface Sci.* **1992**, *152*, 141−160.
(58) Inskeep, W. P.; Silvertooth, J. C. *Soil Sci. Soc. Am. J.* **1988**, *52*, 941−946.
(59) Grossl, P. R.; Inskeep, W. P. *Soil Sci. Soc. Am. J.* **1991**, *55*, 670−675.
(60) Bleam, W. F.; Pfeffer, P. E.; Freye, J. S. *Phys. Chem. Miner.* **1989**, *16*, 809−816.
(61) Cody, G. D.; Mysen, B.; Saghi-Szabo, G.; Tossell, J. A. *Geochim. Cosmochim. Acta* **2001**, *65*, 2395−2411.
(62) Araki, T.; Zoltai, T. *Z. Kristallogr.* **1968**, *127*, 21−33.
(63) Kniep, R.; Mootz, P.; Vegas, A. *Acta Crystallogr. B* **1977**, *33*, 263−265.
(64) Drago, R. S. *Physical Methods for Chemists*, 2nd ed.; Saunders College Publishing: New York, 1992.
(65) Bleam, W. F.; Pfeffer, P. E.; Goldberg, S.; Taylor, R. W.; Dudley, R. *Langmuir* **1991**, *7*, 1702−1712.

Received for review July 12, 2003. Revised manuscript received November 4, 2003. Accepted November 10, 2003.

ES034755S